AIAA JOURNAL
Vol. 39, No. 3, March 2001

Efficient Structural Optimization for Multiple Load Cases Using Adjoint Sensitivities

Mehmet A. Akgün*
Middle East Technical University, 06531 Ankara, Turkey
Raphael T. Haftka†
University of Florida, Gainesville, Florida 32611-6250
K. Chauncey Wu‡ and Joanne L. Walsh§
NASA Langley Research Center, Hampton, Virginia 23681
and
John H. Garcelon¶
Vanderplaats Research and Development, Inc., Colorado Springs, Colorado 80906

Adjoint sensitivity calculation of stress, buckling, and displacement constraints may be much less expensive than direct sensitivity calculation when the number of load cases is large. In general, it is more difficult to implement the adjoint method than the direct method, but it is shown that the use of the continuum adjoint method, along with homogeneity conditions, can alleviate the problem. Expressions for von Mises stress and local buckling sensitivities for isotropic plate elements are derived. Computational efficiency of the adjoint method is sensitive to the number of constraints, and, therefore, the adjoint method benefits from constraint lumping. A continuum version of the Kreisselmeier–Steinhauser functional is chosen to lump constraints. The adjoint and direct methods are compared for three examples: a truss structure, a small high-speed civil transport (HSCT) model, and a large HSCT model. These sensitivity derivatives are then used in optimization.

Introduction

SENSITIVITY of structural response quantities, such as stresses or displacements, to design parameters is useful in optimization, system identification, and probabilistic analysis. Finite difference derivatives are commonly used, but they are expensive computationally and prone to errors. Consequently, there is widespread interest in analytical sensitivity methods, commonly classified as either direct or adjoint methods.[1]

The widely used direct method is obtained by direct differentiation of the equations of equilibrium, which are used to compute the structural responses or static solutions. The number of system solutions required to obtain the constraint derivatives is equal to the product of the number of design variables, the number of load cases, and the number of structural configurations, for example, damaged versions of a structure. The adjoint method is obtained by differentiation of constraint functionals. The number of system solutions required to obtain the derivatives is equal to the number of constraints of interest. For problems with multiple load cases or multiple structural configurations, the adjoint method can be more efficient than the direct method. This computational advantage is enhanced for derivatives of stress functions because these derivatives can be calculated directly rather than obtained from derivatives of the displacements. Reduction of the number of constraints through constraint deletion or lumping enhances the efficiency of the adjoint method.

The computational efficiency of the adjoint method is offset by greater implementation effort compared to the direct method, especially when based on differentiation of discretized structural models. This implementation penalty is alleviated for stress constraints when the adjoint method is implemented based on continuum equations,[2,3] where the adjoint load is implemented as initial strains imposed in the elements of interest.

The objectives of this study are to derive the adjoint initial strains for computing the sensitivity of von Mises stress and local buckling constraints and to demonstrate the efficiency of the adjoint method under multiple load cases with and without constraint lumping. It is shown that buckling and von Mises stress constraints satisfy a homogeneity property that simplifies buckling sensitivity computation by obviating the need to compute partial derivatives of the constraints. A continuum version of the Kreisselmeier–Steinhauser (KS) functional that allows lumping of the constraints with the adjoint method is also investigated. The efficiency of the adjoint method is demonstrated by structural optimization of three problems: a truss structure, a small model of a high-speed civil transport (HSCT), and a large model of an HSCT.

Direct Method

The discretized equations of equilibrium may be written in terms of the stiffness matrix $\boldsymbol{K}$, the force vector $\boldsymbol{f}$, and the displacement vector $\boldsymbol{u}$ as

$$\boldsymbol{K}\boldsymbol{u} = \boldsymbol{f} \tag{1}$$

The recovery of the stress field $\boldsymbol{\sigma}$ from the displacement vector may be written as

$$\boldsymbol{\sigma} = \boldsymbol{S}\boldsymbol{u} \tag{2}$$

where $\boldsymbol{S}$ is the stress-displacement matrix.[4] For a constant load, differentiating Eqs. (1) and (2) with respect to a design variable p we obtain

$$\boldsymbol{K}\boldsymbol{u}_p = \boldsymbol{f}^p \equiv -\boldsymbol{K}_p\boldsymbol{u} \tag{3}$$

$$\boldsymbol{\sigma}_p = \boldsymbol{S}_p\boldsymbol{u} + \boldsymbol{S}\boldsymbol{u}_p \tag{4}$$

where the subscript p is total differentiation with respect to the design variable p and $\boldsymbol{f}^p$ is the pseudoload. The direct method solves for the displacement and stress derivatives from Eqs. (3) and (4), respectively.

Received 27 September 1999; accepted for publication 15 August 2000.

*Associate Professor, Aeronautical Engineering Department; akgun@ae.metu.edu.tr. Member AIAA.
†Distinguished Professor, Department of Aerospace Engineering, Mechanics and Engineering Science; haftka@ufl.edu. Fellow AIAA.
‡Aerospace Engineer; k.c.wu@larc.nasa.gov.
§Aerospace Engineer; j.l.walsh@larc.nasa.gov. Senior Member AIAA.
¶Senior Research and Development Engineer; JohnGarcelon@altavista.com. Member AIAA.

Implementing Eqs. (3) and (4) in finite element software requires a large programming effort for computing derivatives of element stiffness and stress matrices with respect to all possible design variables. An easy-to-implement alternative, known as the semi-analytical method,[5] employs a finite difference evaluation of $\boldsymbol{K}_{,p}$. In addition, we estimate the incremented displacement $\boldsymbol{u}$ with a first-order approximation using the displacement derivative from Eq. (3), which corresponds to a finite difference increment in a design variable. This estimate of $\boldsymbol{u}$ is then used in Eq. (2) to compute the corresponding stresses, and the stress derivative is computed with finite differences, bypassing Eq. (4). The semi-analytical approach is used in the present study. Because the matrix $\boldsymbol{K}$ is available in factored form from solving Eq. (1), the solution for displacement derivatives $\boldsymbol{u}_{,p}$ in Eq. (3) is much cheaper than the solution for the displacements. However, obtaining stress derivatives from displacement derivatives costs about the same as the original stress recovery [Eq. (2)], reducing the savings associated with the direct method compared to a full finite difference calculation of the sensitivity, which involves factoring $\boldsymbol{K}$ a second time.

Adjoint Method

The adjoint method, when formulated directly for a discrete system, tackles derivatives of displacement functionals of the form $g(\boldsymbol{u}, p)$. A stress constraint $g(\boldsymbol{\sigma}, p)$ is converted to a displacement functional as $g(\boldsymbol{Su}, p)$. The derivative of g is given as

$$g_{,p} = g_{,p} + g_{,u} \cdot \boldsymbol{u}_{,p} \tag{5}$$

where a comma denotes a partial derivative with respect to the following subscript and a dot denotes an inner product. With some algebra, Eq. (5) can be converted into

$$g_{,p} = g_{,p} + \boldsymbol{f}^{p} \cdot \boldsymbol{u}^{a} \tag{6}$$

where $\boldsymbol{u}^{a}$ is the adjoint displacement field, found as a solution of the system

$$\boldsymbol{K}\boldsymbol{u}^{a} = g_{,u}^{T} \tag{7}$$

There are implementation difficulties associated with the adjoint method when thusly formulated, which have slowed its widespread application. For stress constraints such as the von Mises equivalent stress, $g_{,u}^{T}$ depends on the stress-displacement relationship and, hence, on the details of the finite elements used. This information is not always readily available. Unlike the direct method, no semi-analytical method is readily available for calculating $g_{,u}^{T}$.

Using a continuum formulation of the adjoint method instead of a discretized formulation can eliminate this problem. The adjoint method for stress constraints then requires the imposition of an adjoint load in the form of an initial strain distribution in the element where the constraint is applied. When the method is applied to a discrete model, an equation of the form

$$\boldsymbol{K}\boldsymbol{u}^{a} = \boldsymbol{f}^{a} \tag{8}$$

has to be solved, where $\boldsymbol{f}^{a}$ is the force equivalent to the adjoint load. A finite element code with initial strain capability can easily generate the adjoint force $\boldsymbol{f}^{a}$.

Continuum Formulation of Constraint Sensitivities

For the continuum approach, a constraint function, for example, a stress or buckling constraint, is more conveniently expressed as a constraint functional G

$$G = \frac{1}{w_0} \int g(\boldsymbol{\sigma}, p)\, \mathrm{d}w \tag{9}$$

where $\boldsymbol{\sigma}$ is a vector of stresses or stress resultants. The integration in Eq. (9) represents an averaging process over an element of the structure with w_0 denoting the size of the element. The sensitivity of G to the design variable p is obtained by differentiating Eq. (9) with respect to p to yield

$$G_{,p} = \frac{1}{w_0} \int \left[g_{,p} + g_{,\sigma} \cdot (\boldsymbol{\sigma}_{,p} + \boldsymbol{\sigma}_{,\varepsilon}\varepsilon_{,p}) \right] \mathrm{d}w \tag{10}$$

When p is a property of a structural element other than the element whose sensitivity is being computed, the partial derivatives with respect to p are zero. For the stress constraint on a truss member, the scalar $\boldsymbol{\sigma}$ is the axial force in the member, and w_0 and $\mathrm{d}w$ represent the total and differential member lengths. For stress or buckling constraints on a plane-stress element, w_0 and $\mathrm{d}w$ are the total and differential plate surface area, and $\boldsymbol{\sigma}$ is the vector of stress resultants $\boldsymbol{N}$, given by

$$\boldsymbol{N} = \begin{bmatrix} N_x \\ N_y \\ N_{xy} \end{bmatrix} = t\boldsymbol{D} \begin{bmatrix} \varepsilon_x \\ \varepsilon_y \\ \varepsilon_{xy} \end{bmatrix} \tag{11}$$

where t is the plate thickness and $\boldsymbol{D}$ is the constitutive matrix. In this case $\boldsymbol{\sigma}_{,p} = \boldsymbol{N}_{,t} = \boldsymbol{N}/t$ when the design variable is the element's own thickness, and $\boldsymbol{\sigma}_{,p} = 0$, otherwise. For a three-dimensional element, $\boldsymbol{\sigma}$ is the stress state and w_0 is the volume. For an isotropic plane-stress element with p being the element's own property ($p = t$), $\boldsymbol{N}_{,t} = \boldsymbol{D}\varepsilon$ and $\boldsymbol{N}_{,\varepsilon} = t\boldsymbol{D}$.

In the continuum formulation, it can be shown[2] that the adjoint load is an initial strain given by $g_{,\sigma}/w_0$, regardless of what p is. Consequently, the loading depends on the constraint functional, but not on the details of the finite element except for its length, surface area, or volume. This loading can be easily applied in any program that has initial strain loading capabilities. The displacement resulting from the application of the adjoint load is called the adjoint displacement $\boldsymbol{u}^{a}$. It can be shown that

$$G_{,p} = \frac{1}{w_0} \int (g_{,p} + \sigma_{,p} \cdot g_{,\sigma})\, \mathrm{d}w + \boldsymbol{f}^{p} \cdot \boldsymbol{u}^{a} \tag{12}$$

where $\boldsymbol{f}^{p}$ is the pseudoload when a finite element model is used [Eq. (3)]. The last term in Eq. (12) is easy to implement, but the integral requires some element level implementation. However, the integrand in Eq. (12), which is in general nonzero when p is the structural element's own property, can be simplified by using a property of homogeneous functions. If g is a homogeneous function of degree h in its arguments, that is, if

$$g(c\boldsymbol{\sigma}, cp) = c^{h} g(\boldsymbol{\sigma}, p) \tag{13}$$

then it can be shown that

$$g_{,\sigma} \cdot (\boldsymbol{\sigma}/p) + g_{,p} = (h/p)g \tag{14}$$

If $\boldsymbol{\sigma}$ is such that

$$\boldsymbol{\sigma}/p = \boldsymbol{\sigma}_{,p} \tag{15}$$

then

$$g_{,\sigma} \cdot \boldsymbol{\sigma}_{,p} + g_{,p} = (h/p)g \tag{16}$$

Equation (15) holds for a truss member and a plate element under in-plane loading, where cross-sectional area and plate thickness are the design variables, respectively. For a plate element, for example, $\boldsymbol{N}_{,t} = \boldsymbol{N}/t$ from Eq. (11). Hence, Eq. (12) becomes

$$G_{,p} = \frac{1}{w_0} \int \left(\frac{hg}{p} \right) \mathrm{d}w + \boldsymbol{f}^{p} \cdot \boldsymbol{u}^{a} \tag{17}$$

When $h = 0$, the integral in Eq. (17) disappears, and the sensitivity is easily calculated. When h is nonzero, Eq. (17) is still easier to calculate than Eq. (12); the integrand is simply a multiple of the function g. Homogeneity of a constraint, hence, does away with the need to implement and compute partial derivatives of the constraint. The constraints for truss and membrane elements have homogeneity properties; thus, we have an additional simplification in the calculation of their derivatives. The homogeneity properties of stress and plate buckling constraints are different and will be studied separately.

Homogeneity of Stress Constraints

A stress constraint on truss members and von Mises constraint on plane-stress elements are homogeneous to the zeroth degree, that is, $h = 0$. These constraints are, thus, unchanged when both the stresses $\boldsymbol{\sigma}$ and the design variable p are scaled up or down by the same factor [Eq. (13)]. The average stress constraint in a truss member is given by

$$G = \frac{1}{L}\int \left(\frac{P}{\Omega\sigma_{\text{all}}} - 1\right) \mathrm{d}L \tag{18}$$

where P is the bar force, L is the length, Ω is the cross-sectional area, and σ_{all} is the allowable stress. Similarly, the average von Mises stress constraint in a plane-stress element is given by

$$G = \frac{1}{A}\int (\sigma_{\text{vM}} - 1)\, \mathrm{d}A \tag{19}$$

where A is the surface area of the plate element. The von Mises stress ratio σ_{vM} is defined by

$$\sigma_{\text{vM}} \equiv \alpha/t\sigma_{yp}, \qquad \alpha^2 \equiv N_x^2 - N_x N_y + N_y^2 + 3N_{xy}^2 \tag{20}$$

and σ_{yp} is the yield stress. In both Eqs. (18) and (19), the integrands are homogeneous to the zeroth degree.

The axial initial strain to be imposed in a bar element to compute the adjoint displacement $\boldsymbol{u}^a$ for the bar stress constraint sensitivity is obtained from Eq. (18) as

$$\varepsilon_{\text{in}} = g_{,P}/L = 1/L\Omega\boldsymbol{\sigma}_{\text{all}} \tag{21}$$

Similarly, the initial strain state to compute the adjoint displacement for a von Mises constraint sensitivity is derived from Eqs. (19) and (20) as

$$\varepsilon_{\text{in}} = g_{,N}^T/A = (1/2\sigma_{yp}At\alpha)(2\boldsymbol{N} - \boldsymbol{N}') \tag{22}$$

where

$$\boldsymbol{N}' \equiv [N_y \quad N_x \quad -4N_{xy}]^T \tag{23}$$

Because of zeroth-order homogeneity, once the displacements due to these initial strains are calculated, the derivatives are given by the last term in Eq. (17).

Homogeneity of Plate Buckling Constraints

An isotropic rectangular flat plate of thickness t and sides a and b may buckle under biaxial loading if the maximum value (over m and n) of

$$1/\lambda_n = -(1/\Delta)\left[N_x(m/a)^2 + N_y(n/b)^2\right] \tag{24}$$

exceeds unity, where an applied stress resultant N_i is positive when tensile and

$$\Delta = \pi^2 t^3 H[(m^2/a^2) + (n^2/b^2)]^2 \tag{25}$$

with

$$H = E/12(1 - \nu^2) \tag{26}$$

An isotropic infinite strip of width b having two simply supported sides, on the other hand, may buckle under pure in-plane shear if

$$\frac{1}{\lambda_s} = \frac{|N_{xy}|b^2}{52.7t^3H} \tag{27}$$

exceeds unity.[6] When Eq. (27) is applied to a rectangular flat plate, b is taken to be the shorter edge. Buckling under combined loading may occur if the value of the interaction equation

$$1/\lambda_{\text{comb}} = (1/\lambda_n) + \left(1/\lambda_s^2\right) \tag{28}$$

reaches unity.[7] Therefore, a buckling constraint for an isotropic plate under combined loading may be written as

$$g(\boldsymbol{N}, t) = g_1(\boldsymbol{N}, t) + g_2(\boldsymbol{N}, t) - 1 \le 0 \tag{29}$$

where $\boldsymbol{N}$ is the vector of stress resultants and

$$g_1(\boldsymbol{N}, t) \equiv 1/\lambda_n, \qquad g_2(\boldsymbol{N}, t) \equiv 1\Big/\lambda_s^2 \tag{30}$$

If λ_n is negative, g_1 is taken to be zero.

The initial strain for the buckling constraint in Eq. (29) is given by $g_{,N}/A$. Hence, assuming $\lambda_n > 0$,

$$\varepsilon_{\text{in}} = \frac{1}{A}\left[-\frac{m^2}{a^2\Delta}, \quad -\frac{n^2}{b^2\Delta}, \quad \frac{2N_{xy}b^4}{(52.7H)^2t^6}\right] \tag{31}$$

Because g does not depend on the position within the plate, it follows from Eq. (12) that

$$G_t = g_t = g_{,t} + g_{,N}\cdot\boldsymbol{N}_{,t} + \boldsymbol{f}^p\cdot\boldsymbol{u}^a \tag{32}$$

when $p = t$ is the thickness of the plate element whose constraint is being evaluated.

As for the homogeneity, the constraint g in Eq. (29) is not homogeneous as a whole, but its components are. For g_1 alone, $h = -2$ and for g_2, $h = -4$. Hence, Eq. (32) becomes

$$G_t = g_t = -(1/t)(2g_1 + 4g_2) + \boldsymbol{f}^p\cdot\boldsymbol{u}^a \tag{33}$$

When t is a property of a structural element other than the plate whose sensitivity is being computed, the buckling sensitivity is simply given by

$$G_t = g_t = \boldsymbol{f}^p\cdot\boldsymbol{u}^a \tag{34}$$

Note that the homogeneity is not limited to the constraints for isotropic plates; it is valid for the total thickness of composite laminates as well, provided the fractional ply thicknesses are kept constant.

Constraint Lumping

Even with constraint deletion, the number of retained constraints may still be large. Reducing the number of constraints by lumping them into groups can increase the savings brought about by the adjoint method. A continuum version of the KS functional is used here to lump a set of constraints for a number of structural elements into a single constraint. The customary form of the KS function replaces a set of l constraint functions

$$g_i(p) \le 0, \qquad i = 1, \ldots, l \tag{35}$$

by

$$\text{KS}[g_i(p)] = \frac{1}{\rho}\ln\sum_{i=1}^{l} e^{\rho g_i(p)} \le 0 \tag{36}$$

In the case of stress constraints, this form can be generalized to a continuum case where the constraint needs to be satisfied over a domain Ω in the structure

$$g(\boldsymbol{x}, p) \equiv [\boldsymbol{\sigma}(\boldsymbol{x}, p)/\sigma_{\text{all}}] - 1 \le 0, \qquad \boldsymbol{x} \in \Omega \tag{37}$$

where $\boldsymbol{\sigma}(\boldsymbol{x}, p)$ may be a principal stress or von Mises stress at point $\boldsymbol{x}$, σ_{all} is the allowable stress, and g may be a buckling constraint as well with g given by Eq. (29). However, the following definition of the KS functional does not depend on the form of g. Namely,

$$\text{KS}[g(\sigma, p)] = g_{\max} + (1/\rho)\ln G[g(\sigma, p)] \tag{38}$$

where $g_{\max}$ is the maximum value of the constraint in the region, ρ is a positive parameter, and

$$G[g(\sigma, p)] = \int \frac{1}{w_0(\boldsymbol{x})}\exp\{\rho[g(\sigma, p) - g_{\max}]\}\, \mathrm{d}\Omega \tag{39}$$

with $1/w_0(\boldsymbol{x})$ being a positive parameter and a weighting function. The term $w_0(\boldsymbol{x})$ may be chosen to emphasize the contribution from certain regions, but is taken constant here. In KS lumping, regions where the constraint is far from being active, that is, the value of g being close to -1, contribute much less to the functional than regions where the constraint is nearly active, that is, the value of g

being close to 0. This may lead to a slightly overweight design as demonstrated in example 1 below. The choice of the value of ρ in the function is therefore important. A small value of ρ leads to an overly conservative KS function while a large value of ρ causes the function to be dominated by the most critical constraints, possibly leading to oscillations in the optimization. For the problems considered here a value of $\rho = 50$ was found to be a good compromise.

The integral in Eq. (39) is taken over all of the elements being lumped together. In the implementation for this study, the integrand in Eq. (39) is constant within each element, and the integral becomes a summation. The derivative of the KS functional is given as

$$\mathrm{KS}_p = G_p/\rho G \tag{40}$$

when $g_{\max}$ is taken as the most critical constraint value among the group of elements and is treated as a convenient constant for the purpose of differentiation. The simplification noted without lumping also holds with KS lumping. For example, for a stress constraint on a bar or a plane-stress element, Eq. (17) applies with $h = 0$. Hence,

$$G_p = \boldsymbol{f}^p \cdot \boldsymbol{u}^a \tag{41}$$

The adjoint displacement $\boldsymbol{u}^a$ is now due to a distribution of initial strain states over the plane-stress or bar elements being lumped. The strain state to be imposed in the ith plane-stress or bar element, simultaneously with the others in the group, is given by

$$\varepsilon^T_{\mathrm{in}_i} = \rho \exp[\rho(g_i - g_{\max})](g_{i,\sigma}/w_{0_i}), \qquad i = 1, \ldots, l \tag{42}$$

In Eq. (42), l is the number of constraints lumped together, and $g_{i,\sigma}/w_{0_i}$ is given by the right-hand side of Eq. (21) or (22), which is the strain state imposed in a single element in the absence of lumping.

For a buckling constraint, steps similar to those leading to Eqs. (32) and (33) from Eq. (12) yield

$$G_p = -\frac{\rho}{p}\sum_{i=1}^{l} \exp[\rho(g_i - g_{\max})](2g_{i1} + 4g_{i2})\delta_{t_i p} + \boldsymbol{f}^p \cdot \boldsymbol{u}^a \tag{43}$$

where $\delta_{t_i p}$ is a Kronecker delta equal to one if design variable p is the thickness of the ith plane-stress element, otherwise it is zero. The initial strain for each plane-stress element is again of the form of Eq. (42) with $g_{i,\sigma}/w_0$ now given by the right-hand side of Eq. (31).

Preliminary Efficiency Comparison

The relative computational efficiencies of the direct and adjoint methods depend on whether or not constraint deletion is used. Without lumping or constraint deletion, the direct method requires solution of Eq. (3) for each design variable, each load case, and each structural configuration, whereas the adjoint method requires the solution of Eq. (8) for each constraint, each load case, and each structural configuration. Even when potentially inactive constraints are deleted before an optimization cycle, or when constraints are lumped, the direct method still requires solution of Eq. (3) for each design variable, each load case, and each structural configuration except for the load cases and configurations with no active constraints. In contrast, the adjoint method now needs to calculate derivatives of only potentially active constraints requiring the solution of Eq. (8) for each such constraint only. The number of active constraints is typically equal to or smaller than the number of design variables. Consequently, when the number of load cases or structural configurations is large, the adjoint method should be more efficient than the direct method. The adjoint method also does not have to go through the stress recovery stage, translating displacement derivatives into stress derivatives. This advantage is eroded by constraint deletion. For large structural problems lumping of the constraints before computing their individual sensitivities increases the relative efficiency of the adjoint method further, as will be shown later.

The lumping strategy used with the direct method was to lump each type of constraints (for example, von Mises or buckling constraints) in a design region under all load cases into a single KS functional. Because an initial strain state could not be found for sensitivity calculation when the constraints under all load cases were lumped into a single functional, a different lumping strategy was used for the adjoint method. The latter strategy was to lump each type of constraint in a design region under the most critical load case into a single KS functional. The most critical load case for a given design region and a given type of constraint is the one that causes the largest constraint value in any element of the region. No ill-conditioning to the optimization was experienced because the constraints associated with each design region (i.e., with elements having a common design variable) were lumped together. No constraint deletion strategy was used with either method with or without lumping. With lumping, the number of constraints was already close to the number of design variables.

Applications

Three examples of varying complexity are used to compare the computational efficiency of the adjoint and direct methods. Example 1 is a 108-bar truss, example 2 is a small HSCT model, and example 3 a large HSCT model. Sensitivity derivatives are obtained using both methods and then used in optimization. The 108-bar truss example is used to compare the adjoint and direct methods with and without lumping. The two HSCT examples are used to compare the two methods as the number of load cases is varied.

Both the adjoint and direct methods are implemented in a commercial finite element program, EAL,[8] for plane-stress elements with von Mises stress constraints and buckling constraints and for truss elements. The optimization code MINOS[9] had been previously incorporated into EAL[10]. The linear programming option of MINOS (based on the simplex method) is used in a sequential linear programming (SLP) optimization approach for this study.

Examples 1 and 2 were run on a single processor Pentium 166-MHz personal computer with a Windows NT operating system at the University of Florida. Example 3 was run on a dual processor Pentium 400-MHz personal computer with a Windows NT operating system at NASA Langley Research Center. For all three examples, the semi-analytical approach described earlier was used to compute the derivative of the stiffness matrix, design variables were constrained by move limits that were initially 50% of the starting design variable values, and when lumping was used the value of the KS functional parameter ρ was 50.

Example 1: 108-Bar Truss

A 45-node, 108-bar, 80-degrees-of-freedom (DOF) plane truss, shown in Fig. 1, was divided into 32 design regions, with bars in each region having a common cross section, thus giving 32 design variables. Optimization runs were made with seven load cases using the direct and the adjoint methods, with and without lumping. When lumping was used, bar stress constraints in each region were lumped into a continuum KS functional. Hence, there were 32 KS functionals in either method. When no lumping was used, there were 756 constraints. The direct method with and without lumping required the solution of Eq. (3) 224 times, with the stiffness matrix already factored, whereas the adjoint method required the solution of Eq. (8), of the same size, 108 and 32 times without and with lumping, respectively. The reason for 108 solutions instead of 756

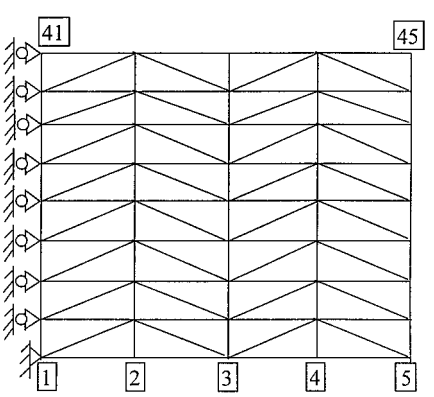

Fig. 1 The 108-bar truss.

Table 1 Optimum weights of the 108-bar truss and total[a] CPU times with the direct and adjoint methods with and without KS lumping under seven load cases

Method	Weight, lb (time, s)
Direct, no lump	36.523 (312)
Direct, lump	37.359 (169)
Adjoint, no lump	36.523 (292)
Adjoint, lump	37.353 (256)

[a]Eight cycles.

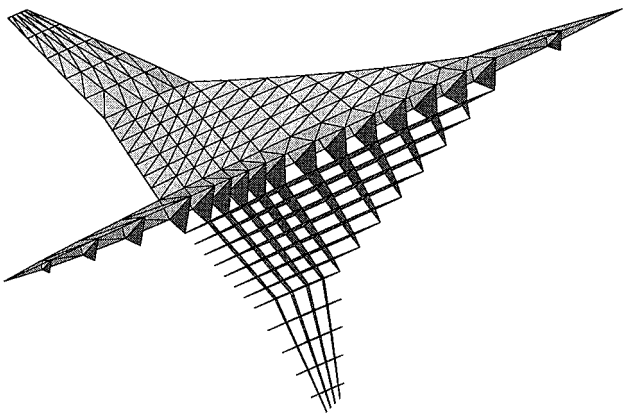

Fig. 2 Small HSCT model.

is that the adjoint load vector $\boldsymbol{f}^a$ for a given bar for different load cases differs only by a scalar factor.

The optimum weight and the CPU time using the adjoint method and the direct method are given in Table 1. The CPU times are for the entire optimization run, that is eight SLP cycles. The optimum weights in Table 1 are the weights at the end of eight optimization cycles representing convergence to 12 significant digits even though only five digits are reported in the table to keep it readable. The direct and adjoint methods agree to 11 digits without lumping and to four digits with lumping.

As can be seen from Table 1, the final weights show some dependence on lumping and the choice of method. This is attributed to optimization history and to the effect of the KS functional, which applies a slightly over-conservative constraint. It can also be seen that the lumping was more beneficial to the direct method than the adjoint method, even though one would expect the opposite. The reason for this anomaly is that the savings associated with the adjoint method is in the solution of the equations of equilibrium with fewer right-hand sides. The cost of this solution increases superlinearly with problem size and is very small for small problems. The additional cost was due to element-level calculations, which is proportional to the number of elements in the problem and is, therefore, more significant than the solution time for small problems.

Example 2: Simple HSCT Model

A simple HSCT wing model, developed by Balabanov et al.,[11] is shown in Fig. 2 (taken from Giunta and Sobieszczanski-Sobieski[12]). The three-dimensional model has 193 nodes, 449 two-node bar elements, 383 triangular isotropic membrane elements, and 129 isotropic shear panel elements with a total of 533 DOF. Not all of the finite elements are designed. There are 40 design variables consisting of 26 membrane thicknesses and 14 bar cross-sectional areas. Skin regions at the trailing edge and strake of the wing are governed by the minimum-gauge-thickness constraint set at 0.0035 ft. The skin thickness within each design region is uniform. The minimum-gauge area used for the bar elements is 0.0040 ft^2.

A series of optimization runs with different numbers of load cases was made. There were five basic load cases due to pull-up maneuvers, climb, cruise, and taxiing. As combinations of the basic five cases, 15 additional load cases were derived. Stress constraints were based on von Mises equivalent stresses in the membrane elements and axial stresses in the bars.

Table 2 Optimum weights of the simple HSCT model and total[a] CPU times; KS lumping used with both methods: W, lb (t, s)

No. of load cases	Direct Method W, lb (t, s)	Adjoint Method W, lb (t, s)
1	119746.9 (750)	119746.9 (1410)
5	149327.1 (1410)	149327.1 (1560)
20	149327.1 (2962)	149327.1 (1627)

[a]Eight cycles.

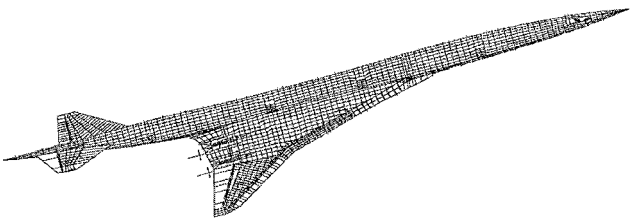

Fig. 3 Half-symmetric finite element model of the large high-speed civil transport.

The model was then optimized under 1, 5, and 20 load cases in different runs subject to buckling and von Mises stress constraints for membrane elements and yield limits for bar elements. Each optimization was run for eight cycles, resulting in convergence of weights to 13 digits. There were 66 KS functions with both methods regardless of the number of load cases. Equation (3) had to be solved a total of 40 times the number of load cases with the direct method and Eq. (8) a total of 66 times with the adjoint method regardless of the number of load cases.

Table 2 shows the optimum weights and the CPU times for the entire optimization run, that is, eight SLP cycles. The final weights from the two methods agree to 13 digits accuracy although only seven digits are reported. Also, for this larger problem, the improved efficiency with number of load cases of this implementation of the adjoint method compared to the direct method is apparent. For 5 load cases the two methods are comparable, and for 20 load cases the adjoint method is about 45% cheaper.

Example 3: Large HSCT model

The third example is a half-symmetric model of an entire high-speed transport aircraft shown in Fig. 3. This model was originally presented by Scotti.[13] Runs were performed at NASA Langley Research Center. The present EAL adjoint runstreams, i.e., set of EAL instructions, cannot handle four-noded membrane elements. Therefore, each such element in the original model's design regions was replaced with two three-noded elements, which increased the total number of elements in the model to 16,434. In addition, all composite honeycomb plate sections were replaced with isotropic membrane sections, which reduced the number of design variables in the model to 61. Both stress and buckling constraints are computed for the triangular elements in the design regions.

There are seven basic load cases: six arising from supersonic maneuvers at $+2.5\ g$ and $-1.0\ g$ and the seventh representing a taxi condition. Additional 14 cases were generated from various combinations of the 6 basic maneuver load cases. For timing purposes, the model was run for four optimization cycles using both the adjoint and direct methods. For each method, analyses were performed with 1, 7, 14, and 21 load cases. Figure 4 shows plots of the actual CPU time required to complete each of the four optimization cycles for the different analysis methods and load case scenarios. The lines in Fig. 4 show the best-fit averages of the run times of the four cycles.

For a single load case, the direct method is twice as fast as the adjoint method. However, as the number of load cases increases, the adjoint method becomes more efficient. Because this example is larger than the earlier two examples, the efficiency of the adjoint method as the number of load cases increases is greater, and the break even point now appears to be around three or four load cases. For 21

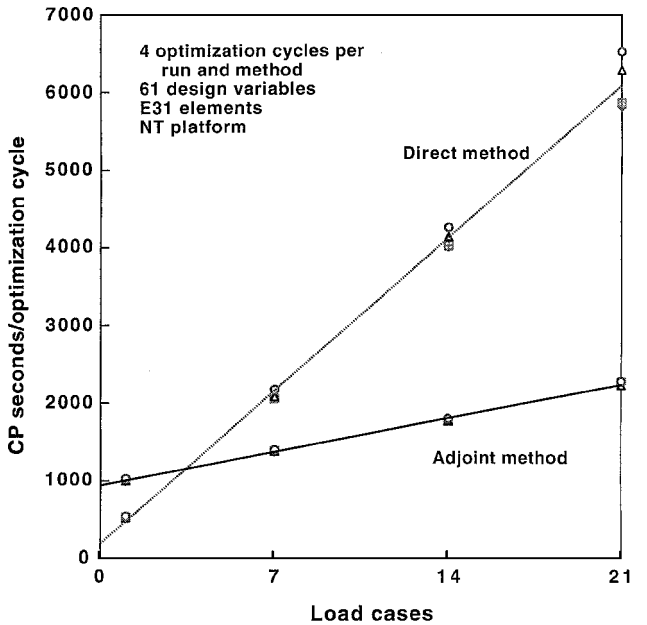

Fig. 4 CPU timing as a function of the number of load cases for the large high-speed civil transport.

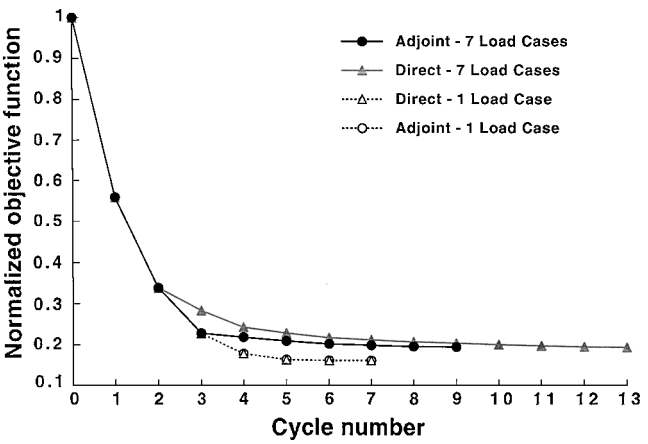

Fig. 5 Optimization history for the large high-speed civil transport.

load cases, the problem solution with the adjoint method requires only about one-third of the time required by the direct method.

In addition, the optimization was run to convergence using both methods with one load case and seven load cases. Figure 5 shows the convergence history for the normalized objective function. It is seen that the direct and adjoint methods converge to comparable weights. The values of the design variables were also similar.

Conclusions

Sensitivities of von Mises stress and normal and shear buckling constraints in membranes have been formulated and computed using the adjoint method. Sensitivity of lumped constraints has also been computed. The present formulation utilizes a characteristic of homogenous functions to avoid calculation of partial derivatives of the constraints and the stress resultants. Test cases, including a 108-bar truss and two HSCT models of different complexities, were used to compare the direct and the adjoint methods of sensitivity computation. The two methods have been compared in terms of efficiency for various numbers of load cases in optimization runs performed with the EAL finite element software.

The direct method was found to be more efficient for optimization of small systems under a small number of load cases. The adjoint method outperforms the direct method in runs with a large number of load cases. The advantage of the adjoint method results from requiring static solutions equal in number to the number of active constraints, whereas the direct method requires a number equal to the number of design variables times the number of load cases. The advantage of the adjoint method increases with problem size because the solution cost per load case increases superlinearly with problem size.

Note, however, that the implemented EAL optimization code was originally developed for the direct method and aided with processors developed especially for this method. The implementation of the adjoint method used standard EAL runstream commands, which may accrue higher overhead during execution. Thus, for a single load case, the adjoint method required substantially more time than the direct method.

No constraint deletion strategy was used with either the direct or the adjoint method. It may be worthwhile to investigate the effect of constraint deletion in conjunction with lumping or without lumping.

Acknowledgments

This work was supported in part by NASA Cooperative Agreement NCC-1-268. The first author acknowledges the fellowship from Turkish Scientific and Technical Research Council that supported part of his visit to the University of Florida and the sabbatical leave of absence granted by Middle East Technical University. The structural model for the example 3 case was supplied by The Boeing Company and the results presented without absolute scales under the conditions of a NASA Langley Research Center property loan agreement, Loan Control Number I22931. Help from V. O. Balabanov from Vanderplaats R&D with the small HSCT model is gratefully acknowledged.

References

[1]Adelman, H. M., and Haftka, R. T., "Recent Developments in Structural Sensitivity Analysis," *Structural Optimization*, Vol. 1, 1989, pp. 137–151.

[2]Haftka, R. T., and Gürdal, Z., *Elements of Structural Optimization*, 3rd ed., Kluwer Academic, Dordrecht, The Netherlands, 1992.

[3]Akgün, M. A., Haftka, R. T., and Garcelon, J., "Sensitivity of Stress Constraints Using the Adjoint Method," *Proceedings of the 39th AIAA/ASME/ASCE/AHS/ASC Structures, Structural Dynamics, and Materials Conference*, AIAA, Reston, VA, 1998, pp. 441–448.

[4]Walsh, J. L., "Application of Mathematical Optimization Procedures to a Structural Model of a Large Finite-Element Wing," NASA TM-87597, 1986.

[5]Camarda, C. J., and Adelman, H. M., "Static and Dynamic Structural-Sensitivity Derivative Calculations in the Finite-Element-Based Engineering Analysis Language (EAL)," NASA TM-85743, 1984.

[6]Whitney, J. M., *Structural Analysis of Laminated Anisotropic Plates*, Technomic, Lancaster, PA, 1987, p. 121.

[7]Lekhnitskii, S. G., *Anisotropic Plates*, translated by S. W. Tsai and T. Cheron, Gordon and Breach Science, New York, 1968, p. 476.

[8]Whetstone, W. D., "EISI-EAL Engineering Analysis Language Interim Release, EAL/325 User Instructions, Version 325.05," Engineering Information Systems, San Jose, CA, Jan. 1990.

[9]Murtagh, B. A., and Saunder, M. A., "MINOS 5.4 User's Guide (preliminary)," Systems Optimization Lab., TR. SOL 83-20R, Stanford Univ., Stanford, CA, 1983 (revised 1993).

[10]Martin, Jr., C. J., "Documentation for a Structural Optimization Procedure Developed Using the Engineering Analysis Language (EAL)," NASA CR-201632, 1996.

[11]Balabanov, V. O., Kaufman, M., Giunta, A. A., Haftka, R. T., Grossman, B., Mason, W. H., and Watson, L. T., "Developing Customized Wing Weight Function by Structural Optimization on Parallel Computers," *Proceedings of the 37th AIAA/ASME/ASCE/AHS/ASC Structures, Structural Dynamics and Materials Conference*, Pt. 1, AIAA, Reston, VA, 1996, pp. 113–125.

[12]Giunta, A. A., and Sobieszczanski-Sobieski, J., "Progress Toward Using Sensitivity Derivatives in a High-Fidelity Aeroelastic Analysis of a Supersonic Transport," *Proceedings of the 7th AIAA/USAF/NASA/ISSMO Symposium on Multidisciplinary Analysis and Optimization*, Pt. 1, AIAA, Reston, VA, 1998, pp. 441–453.

[13]Scotti, S. J., "Structural Design Using Equilibrium Programming Formulations," NASA TM-110175, 1995.

E. R. Johnson
Associate Editor